

M. Clever, G. Arnoux, N. Balshaw, P. Garcia-Sanchez, K. Patel,
G. Sergienko, D. Soler, M. Stamp, J. Williams, K.-D. Zastrow
and JET EFDA contributors

A Wide Angle View Imaging Diagnostic with All Reflective, In-Vessel Optics on JET

“This document is intended for publication in the open literature. It is made available on the understanding that it may not be further circulated and extracts or references may not be published prior to publication of the original when applicable, or without the consent of the Publications Officer, EFDA, Culham Science Centre, Abingdon, Oxon, OX14 3DB, UK.”

“Enquiries about Copyright and reproduction should be addressed to the Publications Officer, EFDA, Culham Science Centre, Abingdon, Oxon, OX14 3DB, UK.”

The contents of this preprint and all other JET EFDA Preprints and Conference Papers are available to view online free at www.iop.org/Jet. This site has full search facilities and e-mail alert options. The diagrams contained within the PDFs on this site are hyperlinked from the year 1996 onwards.

A Wide Angle View Imaging Diagnostic with All Reflective, In-Vessel Optics on JET

M. Clever¹, G. Arnoux², N. Balshaw², P. Garcia-Sanchez³, K. Patel²,
G. Sergienko¹, D. Soler⁴, M. Stamp², J. Williams², K.-D. Zastrow²
and JET EFDA contributors*

JET-EFDA, Culham Science Centre, OX14 3DB, Abingdon, UK

¹*Institute of Energy and Climate Research - Plasma Physics, Forschungszentrum Jülich GmbH,
Association EURATOM-FZJ, 52425 Jülich, Germany*

²*EURATOM-CCFE Fusion Association, Culham Science Centre, OX14 3DB, Abingdon, OXON, UK*

³*Laboratorio Nacional de Fusion, Asociacion EURATOM-CIEMAT, Madrid, Spain*

⁴*Winlight System, 135 rue Benjamin Franklin, ZA Saint Martin, F-84120 Pertuis, France*

** See annex of F. Romanelli et al, "Overview of JET Results",
(23rd IAEA Fusion Energy Conference, Daejeon, Republic of Korea (2010)).*

Preprint of Paper to be submitted for publication in Proceedings of the
27th Symposium on Fusion Technology (SOFT), Liege, Belgium
24th September 2012 - 28th September 2012

ABSTRACT

A new wide angle view camera system has been installed at JET in preparation for the ITER-like wall campaigns. It considerably increases the coverage of the vessel by camera observation systems and thereby helps to protect the - compared to carbon - more fragile plasma facing components from damage. The system comprises an in-vessel part with parabolic and flat mirrors and an ex-vessel part with beam splitters, lenses and cameras. The system delivered the image quality required for plasma monitoring and wall protection.

1. INTRODUCTION

Imaging systems at JET are extensively used for plasma monitoring, plasma wall interaction studies and - since the installation of the more fragile, beryllium and tungsten ITER-like wall (ILW) [1] - for protection of the plasma facing components (PFC) [2]. Two wide angle view systems were already installed at JET before the ILW. For maximising the coverage of the beryllium first wall with protection cameras, a third wide angle view system was required and installed prior to the start of the experimental campaigns in October 2011. Due to the chosen location, the new system ideally complements the existing two systems in that it views the vessel in the opposite toroidal direction and thereby enables the observation of the limiter side subject to the impact of fast ions and re-ionised neutrals injected by the heating system. The time (one year) and budget constraint forced us to develop a new concept simpler than a periscope tube, with in-vessel optical components.

2. OPTICAL AND MECHANICAL DESIGN

The system is composed of two parts, an in-vessel part, which we call the mirror box, and an ex-vessel part comprising beam splitters, cameras and lenses. The vacuum interface between the two parts is composed of a double window made of fused silica. In contrast to the other wide angle view systems at JET, the design of the new system does not use a periscope tube to hold the optical components and transport the beam. This reduces the price of manufacturing and enabled an implementation without interfering with the neutron diagnostic line of sight through the main port (see figure 2).

The mirror box (figure 2b) is attached to the vacuum vessel wall on the low field side of the torus. The mirror system is made up of a lower and an upper branch, each viewing half of the machine through a conically shaped pupil with a minor diameter of 3mm (figure 2c). A 30 o-axis parabolic mirror with a focal length of 50.8mm then creates an intermediate image of the object inside the box close to the surface of the second, flat mirror. The half images of the two branches are then combined on the camera sensor to form a full wide angle view image. The exit aperture of the box is 80mm by 60mm. The whole box is about 200mm high, 100mm wide and 76mm deep. Figure 1 shows a picture of the mirror box with the intermediate image inside the rectangular exit aperture.

Since the mirrors are exposed to high heat fluxes (thermal cycles up to 400C are expected) and in order to reduce the electromagnetic forces, the mirrors were made from stainless steel and coated with rhodium. The rhodium coating was chosen for its good reflectivity in the visible (>75%) and

nearinfrared spectral range (85% at 1016nm), as well as for its good adherence to stainless steel [3]. Furthermore this material combination choice was also made because it is thought to be a suitable candidate for diagnostic mirrors in ITER. For the flat mirrors, the rhodium coating was applied directly to the polished stainless steel surface, whereas for the parabolic mirrors a 100 μ m amorphous electroless coating of a nickel-phosphorus alloy was used on the polished stainless steel surface to reduce surface micro roughness after polishing and allow for more accurate surface shaping.

Apart from the two entrance pupils in the front and the exit window in the back, the mirror box is completely closed (the side plate is not shown in figure 2 b) for illustrational purposes only). This closed geometry towards the plasma aims to protect the mirrors from erosion due to charge-exchange neutrals, helping to maintain the reflectivity of the mirrors. Furthermore, the all-reflective in-vessel design was also chosen for the system to be less subject to optical degradation due to neutron irradiation compared to a system based on radiation transmitting elements. Due to the closed geometry of the box, the mirrors are expected to be - if at all noticeably affected - deposition-dominated, with the deposition dominantly consisting of beryllium. However, experience in the degradation of the optical properties of mirrors in magnetic fusion devices so far is based on machines with substantial carbon inventory [4, 5]. First mirror tests in the all-metal JET machine have only just started with the first ILW campaign. Previous experiments in the linear plasma device PISCES-B have shown, that the properties of beryllium deposits and their effect on the optical properties of the system will strongly depend on the deposition conditions, i.e. temperature and neutral pressure at the mirror location [6]. For the mirror box, deposition is expected to be low and so far no significant degradation in the transmission of the system in the visible and near-infrared spectral range could be observed. For remote handling to be able to operate with its full capability, the mirror box has to be temporarily removed during the current shutdown. This will enable a visual inspection of the mirror surfaces to be carried out which will give further insight into the effects of the experimental campaign on the mirror box.

The ex-vessel part of the system is composed of two 50/50 beam splitters at 45°, three CCD cameras and three telephoto zoom lenses set to a focal length of 250mm (figure 2a). An unfiltered colour CCD camera provides video images for general plasma operation monitoring in the visible spectral range. Two monochrome CCD cameras equipped with near-infrared interference filters monitor temperatures of the PFCs as part of the protection system for the ILW [2]. The cameras therefore record thermal emission at a wavelength of 1016 nm \pm 40 nm. The choice of a zoom lens with a focal length range from 75mm to 300mm has proven extremely beneficial for camera alignment. The front of these lenses is about 2480mm from the intermediate image inside the mirror box, where the images of the two entrance pupils are formed and perfectly overlap.

3. IMPLEMENTATION AND ALIGNMENT

For the in-vessel part, the implementation of the diagnostic involved the use of manual as well as remote handling. In a first step a mounting block was welded to the vessel wall during a man

entrance into the JET vacuum vessel (yellow part in figure 2b). The remainder of the installation was then carried out by remote handling.

The correct positioning of the mirror box inside the vessel is crucial to ensure maximum transmission and an optimised viewing angle of the system. Hence, the alignment of the box was tested and horizontal and vertical tilt angle corrections measured using a dedicated alignment bracket (figure 3). This bracket was temporarily fixed to the mounting block by remote handling and then viewed from outside the vessel through the diagnostic port using a CCD camera. The position and orientation of the camera were adjusted so that it was looking along the optical axis defined by the centre of the port window and the centre of the convex mirror mounted at the rear plate of the alignment bracket. Two different methods were then used to determine the tilt angles with respect to the known orientation of the alignment bracket. The uncertainty of these alignment methods was required to be not more than 0.5° in vertical and horizontal directions.

The convex mirror method: A small light diode was fixed on the optical axis in front of the camera lens and its reflection in the convex mirror was then used to determine the tilt angles. Figure 4 shows a sketch of this method. If the tilt angle ϕ is small, it can be calculated from the displacement y of the diode in the recorded image with respect to the centre of the mirror based on the following formula:

$$\phi \approx \arctan\left(y \cdot \frac{L - d_{\text{cross}}}{L \cdot d_{\text{cross}}}\right)$$

Here $R = 258.4\text{mm} \pm 0.05\%$ is the radius of the convex mirror curvature and $L = (2366 \pm 50)\text{mm}$ the distance between the diode and the mirror. The centre of the mirror in the image is determined by fitting an ellipsis to the edge of the mirror. This centre \tilde{C} deviates slightly from the point C used to derive the above formula. However, due to the small tilt angle the deviation is negligible compared to the other measurement uncertainties. Note that this method may suffer from back reflection of the light diode on the double window. Luckily the reflected spot did not overlap with the image of the diode from the convex mirror. Because of that risk, an alternative method was developed.

The cross wire method: The position of a cross wire fixed inside the front face of the alignment bracket in relation to markings on the rear plate were used to determine the horizontal and vertical tilt angles. In this case the tilt angle ϕ was determined from the displacement y of the cross wire, the distance L to the rear plate (see above) and the distance between cross wire and rear plate $d_{\text{cross}} = (286.5 \pm 1)\text{mm}$ according to the following formula:

$$\phi \approx \arcsin\left(y \cdot \frac{L + R}{L \cdot R}\right)$$

With an uncertainty of 5mm in the alignment of the camera (and the diode) on the optical axis of the system, the uncertainty of both methods in the determination of the tilt angle is $\pm 0.25^\circ$. It is therefore well within the desired tolerance. The values determined by the two methods agreed well within this uncertainty and were then used to manufacture the attachment bracket for the mirror

box. The box was attached and finally installed in the vessel using remote handling.

The alignment procedure for the in-vessel box also enabled the determination of the correct location of the ex-vessel optics and cameras in relation to the diagnostic port. Based on these measurements a closed box was designed to hold the exvessel optics thereby protecting them from dust, damage and stray light.

4. CALIBRATION, VALIDATION AND PERFORMANCE

In order to use the two filtered CCD cameras for temperature measurements as part of the protection system for the ILW, a calibration and validation had to be performed. The ex-vessel part was calibrated in the lab using a calibrated hot source [7]. A temperature lookup table was then calculated taking into account the nominal transmission of the mirror box based on the measured reflectivity of the mirrors (see section 2), the transmission of the vacuum window and the emissivity of the monitored material [2].

The second step in the commissioning procedure is the validation of the temperature measurements by performing a cross comparison with another temperature measurement, in this case that of a thermal IR camera (measuring at a wavelength of $4\mu\text{m}$) [7]. Figure 5 shows a comparison between the temperature measured by the IR camera (KL7) on a wide outer poloidal limiter (WOPL) and the temperatures at two further WOPL surfaces measured by one of the filtered CCD cameras of the presented system (i.e. at the same poloidal but different toroidal location). Apart from a considerable difference in the lower temperature threshold of the two cameras, the measured temperatures agree within the accepted tolerance of $\pm 50^\circ\text{C}$ for the protection system. A strong toroidal asymmetry in the peak temperature can however be observed, with WOPL7B apparently getting considerably hotter than 8B and 1D.

The system also allowed to observe for the first time in a tokamak the impact of ions on the beam "re-ionisation" tiles installed at the outer wall [8]. These ions stem from the reionisation of neutrals - injected by the neutral beam heating system - in the plasma edge outside the separatrix.

During the installation as well as the operation of the system, a few issues have become apparent: The optical design (i.e. the long focal length) together with the construction of the ex-vessel box make it very difficult to properly align the cameras. Furthermore, due to the long focal length and the use of a zoom lens, which has moveable internal parts that are hard to fix properly, the system is very susceptible to vibrations (figure 6). A fixed focal length lens would reduce the sensitivity to vibrations, but would increase the difficulty in aligning the system. Although the mirror box does not seem to have suffered otherwise from its location inside the vessel, a crack has appeared on the flat mirror of the upper branch quite early in the operational stage (figure 6 a)). The crack, however, has not changed since then and is thought to be only in the coating, coming from excess of stress at this location or bad adhesion. Furthermore, the beamsplitters were not optimised for the system leading to ghost images. They will be replaced by thinner, anti-reflection coated substrates during the current shutdown.

CONCLUSION

The system delivered the imaging quality required for protection of the ILW and does not seem to have suffered too much from plasma-mirror interaction.

How important the development of this new wide angle view system for JET was - and indeed how necessary a further increase in the coverage of the wall - has become evident in a recent experiment. There, significant toroidal asymmetries in limiter temperatures have been observed (figure 5), leading to some beryllium limiters not observed by the protection system to reach melting point while toroidally 'equivalent' surfaces stayed below. It is therefore good news that a further wide angle view system similar to the one presented in this paper is currently under development at JET.

ACKNOWLEDGEMENTS

This work, supported by the European Communities under the contract of Association between EURATOM and CCFE, was carried out within the framework of the European Fusion Development Agreement. The views and opinions expressed herein do not necessarily reflect those of the European Commission. This work was also part-funded by the RCUK Energy Programme (Grant No. EP/I501045).

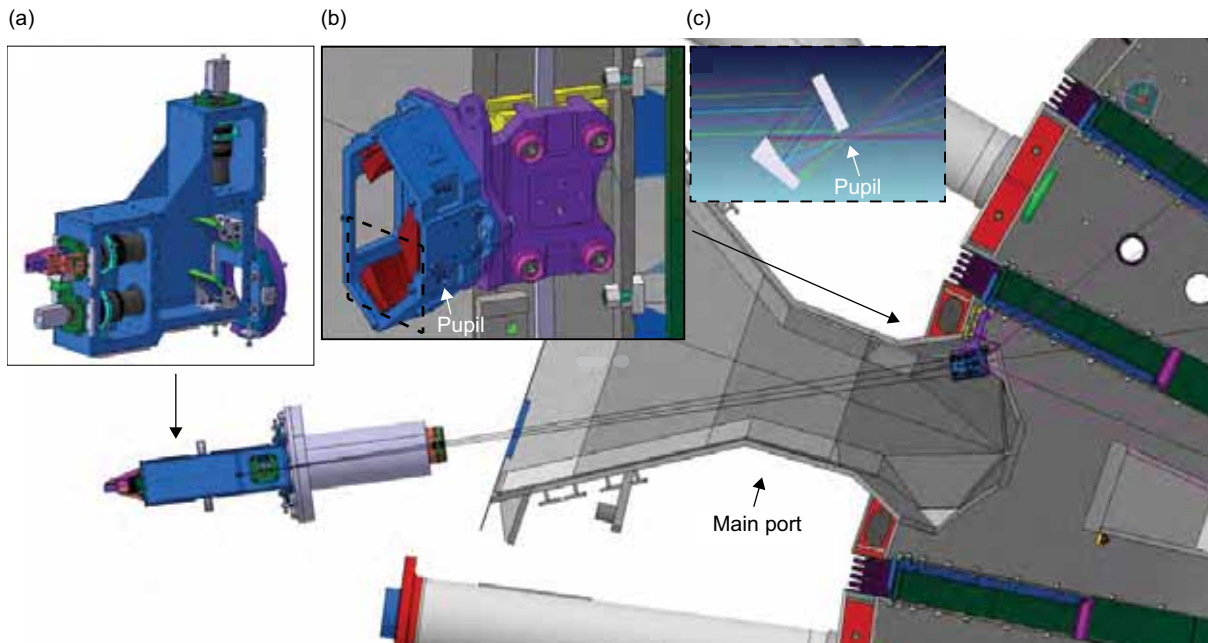
REFERENCES

- [1]. G. F. Matthews, et al., *Physica Scripta* 2011 **T145** (2011) 014001. doi:10.1088/0031-8949/2011/T145/014001.
- [2]. G. Arnoux, et al., *Review of Scientific Instruments* **83** (10) (2012) 10D727. doi:10.1063/1.4738742.
- [3]. L. Marot, et al., *Thin Solid Films* **516** (21) (2008) 7604 – 7608. doi:10.1016/j.tsf.2008.04.087.
- [4]. A. Litnovsky, et al., *Nuclear Fusion* **49** (7) (2009) 075014. doi:10.1088/0029-5515/49/7/075014.
- [5]. M. Rubel, et al., *Physica Scripta* 2011 **T145** (2011) 014070. doi:10.1088/0031-8949/2011/T145/014070.
- [6]. G.D. Temmerman, et al., *Journal of Applied Physics* **102** (8) (2007) 083302. doi:10.1063/1.2798389.
- [7]. I. Balboa, et al., *Review of Scientific Instruments* **83** (10) (2012) 10D530. doi:10.1063/1.4740523.
- [8]. M.L. Mayoral, et al., in: 24th IAEA Fusion Energy Conference, 2012.



JG12.300-1c

Figure 1: In-vessel mirror box with intermediate image showing a wide angle view of the inside of the JET vacuum vessel (upside down).



JG12.300-2c

Figure 2: Schematic view of the system from the top showing the optical path. Inset a) shows the ex-vessel part, inset b) shows the mirror box (blue) including its fixation to the vacuum vessel (purple and yellow). The mirrors are shown in red. Inset c) shows the optical path for the lower branch inside the mirror box (indicated in b) by the dashed box).



Figure 3: Alignment bracket prior to installation. The convex mirror in the rear plate was used to determine corrections to the horizontal and vertical tilt. The cross wires in the front plate together with markings on the rear plate provided a second independent measurement.

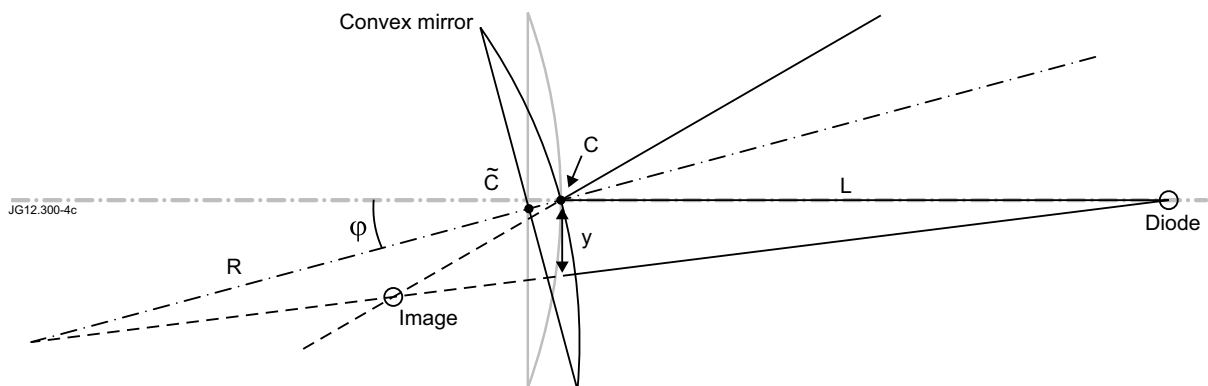


Figure 4: Sketch of the alignment method using a convex mirror and a diode to determine the tilt angles. The tilt ϕ leads to a displacement y of the image of the diode with respect to the centre of the mirror. The angle can be calculated from y provided the curvature R of the mirror and the distance L between diode and mirror are also known. Further details are given in the text.

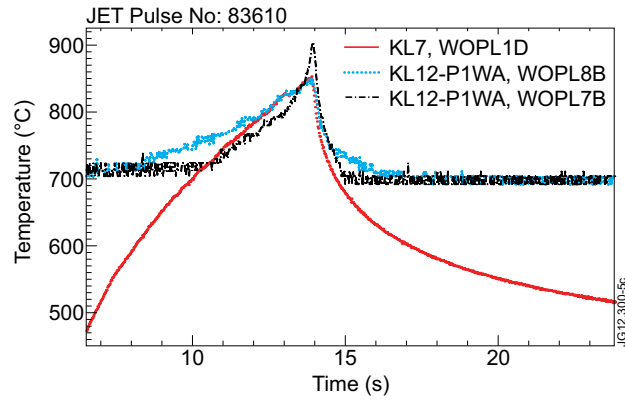


Figure 5: Cross comparison of temperature measurement on outer poloidal limiters from one of the filtered CCD cameras (KL12-P1WA) and from a thermal IR camera (KL7).

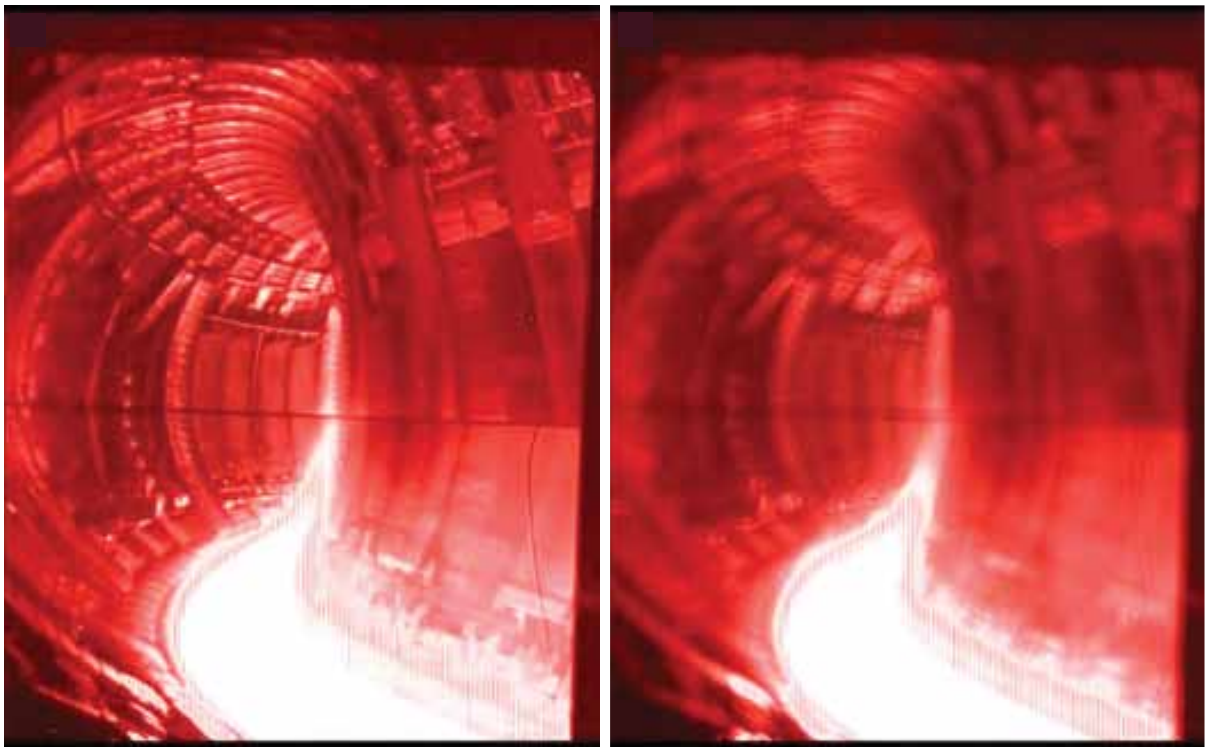


Figure 6: Two images from JET Pulse No: 82631 taken by the colour camera illustrating the effect of the vibrations on the recorded images. Figure a) shows frame 583 with the crack visible in lower right hand side of the image, while b) shows a typical blurred image (frame 575).